Carbohydrate Polymers 88 (2012) 232–238

Contents lists available at SciVerse ScienceDirect

Carbohydrate Polymers

journal homepage: www.elsevier.com/locate/carbpol

Stable nanomicelles based on chitosan derivative: *In vitro* antiplatelet aggregation and adhesion properties

Gang-Biao Jiang[a,*,1], Zuan-Tao Lin[a,1], Xiao-Jun Xu[b], Hai Zhang[c], Kui Song[b,*]

[a] Department of Pharmaceutical Engineering, South China Agricultural University, Guangzhou 510642, China
[b] Department of Hematology, Zhongshan Hospital, Sun Yat-sen University, Zhongshan 528403, China
[c] Department of Ultrasound, Shenzhen People's Hospital, the Second Clinical colloge of Jinan University, Shenzhen 518020, Guangdong Province, China

ARTICLE INFO

Article history:
Received 30 September 2011
Received in revised form
25 November 2011
Accepted 30 November 2011
Available online 9 December 2011

Keywords:
Antiplatelet aggregation and antiplatelet adhesion
Chitosan
Nanoparticles
Polymer–drug conjugate

ABSTRACT

Amphiphilic chitosan derivative (SA-chitosan), water insoluble chitosan modified with salicylic acid (SA), possessed both antiplatelet aggregation and adhesion properties. Chemical structure was characterized by FTIR and ^{1}H NMR. The SA substitution degree calculated by ^{1}H NMR was 70.8%. SA-chitosan can form micelles (size: 292 ± 2 nm). The Critical aggregation concentration (CAC) value (1.216×10^{-4} mg/mL) and zeta potential (52 mV) indicated that they had excellent dispersion stability. TEM image suggested that the micelles were almost spherical. The result of *in vitro* antiplatelet activity revealed that the potential platelet aggregation inhibitory activity by different agonists was in a dose-dependent manner. At low SA-chitosan concentrations, antiplatelet aggregation capability of SA-chitosan was better than that of low-dose aspirin. The platelet adhesion test showed significant difference between the effect of SA-chitosan and that of the control group ($p < 0.05$). These results indicated that SA-chitosan can be potentially used as an antiplatelet aggregation and adhesion agent.

© 2011 Elsevier Ltd. All rights reserved.

1. Introduction

Salicylic acid (SA), the forerunner of aspirin (acetyl-salicylic acid), is a significant hydroxybenzoic acid with anti-inflammatory, pain-relieving, analgesic, astringent, anti-rheumatic and anticarcinogenic properties. However, the therapeutic use of SA is limited by its poor solubility and digestive problems, such as gastro-enteric mucosa irritation. Accordingly, great endeavors have been devoted to overcome these disadvantages. As well known, aspirin, a widely used drug, presents the properties of anti-inflammatory and antiseptic, as well as inhibits platelet aggregation in clotting blood process. Thus, it is widely utilized to decrease the risk of arterial thrombosis by selectively blocking important platelet enzymes or receptors, and to prevent myocardial infarction and treatment of unstable angina (Bryers et al., 2006; Patrono, Rodriguez, Landolfi, & Baigent, 2005). However, it would show mucosa irritation to some extent if one takes the oral aspirin for a long time, and it is poor water-soluble. In addition, it has given rise to an intractable problem, namely, aspirin resistance that has been observed in patients with coronary artery disease. Depending on different definition of aspirin resistance, the prevalence of aspirin resistance can range from 5.5% to 60% (Takahashi et al., 2007). Therefore, new strategies that can reduce side effect and improve the solubility of antiplatelet agents based on salicylic acid are expected.

Recently, polymer micelles which are formed by self-aggregation of bio-degradable copolymers or grafting polymers to be employed as versatile vehicles, have been gained universal attention in pharmaceutical and biomedical fields in view of their distinct characters, such as small size and shell–core structure. Their minute size can avoid the recognition and clearance by mononuclear phagocyte, enhance the penetration of biological membranes, and prolong the circulation half-life, making them suitable for systemic administration and bringing about reduction in the frequency of drug use (Kwon & Okano, 1996; Wiraharma, Zhang, Venkataraman, Hedrick, & Yang, 2009; Zhang et al., 2008). Therefore, several studies about antiplatelet agents were reported. For instance, aspirin was solubilized through polymer micelles, but their high operate cost would limit its further application in pharmaceutical industry (Kumar, Muzzarelli, Muzzarelli, Sashiwa, & Domb, 2004). Shrivastava et al. (2009) reported that the silver nanoparticles had antiplatelet properties, but their antiplatelet adhesion property had not been investigated. On the other hand, in particular, considering the biocompatibility and biodegradability, increasing attention has been paid to the natural abundant polymer. However, few reports utilized natural polymer or their derivatives to act as an antiplatelet aggregation and antiplatelet adhesion agent.

* Corresponding authors. Tel.: +86 20 85280292/760 88873385.
E-mail addresses: jgb3h@163.com (G.-B. Jiang), songkui2001@163.com (K. Song).
[1] These authors contributed equally to this work.

0144-8617/$ – see front matter © 2011 Elsevier Ltd. All rights reserved.
doi:10.1016/j.carbpol.2011.11.089

Chitosan, a natural biodegradable, biocompatible and non-toxic cationic polysaccharide, is derived from chitin, but it is water-insoluble. However, its plentiful free amino groups made it available for preparing a series of polymer micelles with excellent performance and unique properties via introduction of various hydrophobic and/or hydrophilic groups. Thus, tremendous effort has been offered to the chemical modification of chitosan to improve its soluble property, and there is increasing interest in employing chitosan and its derivatives as potent drug delivery and diverse devices in biomedical engineering (Kumar, 2000; Kumar, Chen, et al., 2004; Martin et al., 2002; Muzzarelli et al., 2012).Medicaments based on chitosan derivatives or other polymers having both antiplatelet aggregation and antiplatelet adhesion function simultaneously are not known. Scope of the present paper is the preparation and the characterization of water-soluble polymeric micelles based on chitosan modified with salicylic acid.

2. Materials and methods

2.1. Materials

Chitosan (M_W 250 kD, degree of deacetylation = 90%) was purchased from Sanland Chemical Co., Ltd. (Los Angel, USA). Salicylic acid was provided by Tianjin Chemical Co., Ltd. (Tianjin, China). DAMP, pyrene and *N*-(3-dimethylaminopropyl)-*N*′-ethylcarbodiimide hydrochloride (EDC) were obtained from Sigma (St. Louis, MO). All chemicals were of analytical grade and were used without further purification. The water used was double distilled water.

2.2. Preparation of SA-chitosan

2.0 g of chitosan was dissolved in 200 mL of 1% acetic acid solution, and was diluted with 200 mL ethanol, followed by the addition of certain amount of salicylic acid. Afterward, EDC and DAMP were added. The resultant mixture was keep stirring for 24 h, followed by removal of ethanol at 45 °C under vacuum distillation, then lyophilized. Finally, the product was washed with ethanol for several times to removed the unreacted salicylic acid, EDC and DMAP, and dried under vacuum at 45 °C.

2.3. Instrumental analyses

Fourier transform infrared (FT-IR) spectra of the polymer samples were recorded on a Nicolet 6700 Infrared Detector (Thermo Fisher Scientific, USA). Dry powder of chitosan, SA-chitosan, salicylic acid/chitosan mixture (50%, w/w) and salicylic acid were mixed with KBr, and were pressed to a plate for measurement.

^{1}H NMR spectra were obtained by using a Bruker AV-600 MHz spectrometer (Bruker Analytik GmbH, Germany). Chitosan was dissolved in a mixed solvent of CCl_3COOD and D_2O, while SA-chitosan was dissolved in D_2O to get spectrum of polymer micelles. Salicylic acid was dissolved in DMSO.

The substitution degree of salicylic acid was calculated by the ^{1}H NMR spectrum of SA-chitosan. The ratio of the intensity of the peak at δ = 6.97–7.84 ppm (aromatic ring protons of salicylic acid) to that at δ = 3.04 ppm (H-2 protons of chitosan) was used to evaluate the substitution degree of salicylic acid, which was defined as the number of aromatic ring groups per 100 sugar residues of chitosan (Jiang, Quan, Liao, & Wang, 2006; Liu, Chen, Lin, & Liu, 2006).

TG curves were obtained using a TG 209 F3 Tarsus (Netzsch, Germany) under a flow of nitrogen gas.

Fluorescence spectra were investigated by using a F-4500 FL Spectrophotometer (Hitachi, Japan) at 20 °C. The sample solution was performed prepared as the following method (Kwon et al., 2003): 20 mg of SA-chitosan was dissolved in 10 mL of double distilled water, then was sonicated.

The pyrene was dissolved in tetrahydrofuran (THF) (3.0×10^{-2} M). The pyrene solution was diluted with certain amount of double distilled water and the THF was removed under vacuum at 30 °C for 2 h to obtain the pyrene concentration of 1.2×10^{-6} M. A pyrene concentration in the final sample solution of 6.0×10^{-7} M, this solution was mixed with the same volume of SA-chitosan solutions, resulting in the final sample solution with a pyrene concentration (6.0×10^{-7} M). The concentrations of sample solutions were in the range from 1.6×10^{-3} mg/mL to 2.56×10^{-7} mg/mL. The spectra of pyrene emission were obtained to measure the CAC of SA-chitosan micelles. The excitation (λ_{ex}) and emission (λ_{em}) wavelengths were set at 336 nm and 456 nm, and the slit widths for emission and excitation were at 2.5 nm and 10.0 nm, respectively, while the scan speed was set at 240 nm/min.

The size and zeta potential of the SA-chitosan micelles were measured by using a dynamic light scattering (DLS) measurement at 25 °C on a Zetasizer 3000 HS/HPL (Malvern Instruments Co., Ltd., UK). Sample solutions were dissolving 10 mg of SA-chitosan power into 10 mL double distilled water, followed by the filtration through a 0.45 μm syringe filter.

2.4. Morphology

The morphology of SA-chitosan micelles was observed by using TEM image on a JEM1400 electron microscope (JEOL, Japan). SA-chitosan was dissolved in double distilled water, followed by placing a drop of sample solution onto a 200 mesh copper grid coated with carbon, and then removed surface water with a filter paper, finally, air-dried for 5 min. The micelles were deposited on the grid, then the application of methylamine tungstate negative staining for 2 min.

2.5. In vitro platelet aggregation assay

Blood samples were taken from healthy volunteers who had not taken any drugs during the 2 weeks prior to blood sampling. Blood (ethical approval was obtained from Zhong Shan Hospital, Sun Yat-sen University) was collected into buffered sodium citrate (3.8%, w/v) pH 6.5 as the anticoagulant at a ratio of 9:1 (v/v) and used within 3 h of collection. Aggregation was measured by electrical impedance method. An aliquot of whole blood (0.5 mL) was diluted with an equivalent volume of isotonic saline and incubated for 5 min at 37 °C. The impedance of each sample was monitored in sequential 1-min intervals until a stable baseline was established (<5 mV drift per minute). After a stable baseline was established, the agonists including ADP (10 μM), AA (10 μM) as well as collagen (50 mg/L) were then added to the sample, aggregation were monitored for 6 min, and the final increase in ohms over this period was displayed as a numeric LED readout. The tested compounds of SA-chitosan, including aspirin, were assayed at various concentrations (10, 20 and 50 mg/L). The experiments were carried out in triplicate.

2.6. Platelet adhesion test

Platelet adhesiveness *in vitro* in human was determined by a global glass rotation method. Briefly, blood was drawn from healthy volunteer (ethical approval was obtained from Zhong Shan Hospital, Sun Yat-sen University). The anticoagulant was trisodium citrate 3.8%, 1 part to 9 parts of blood. 1.5 mL citrated control sample or blood containing 50 mg/L SA-chitosan was rotated in a standard glass bottle at room temperature for 15 min at 3 rpm. Then, 1 mL blood was transferred to a tube containing 19 mL solution of sodium citrate. After 2 h, the supernatants tested for platelet count. The

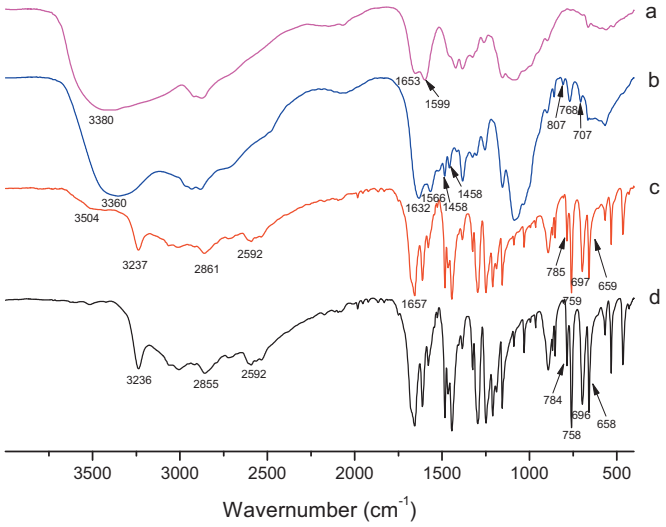

Fig. 1. FT-IR spectra: (a) chitosan; (b) SA-chitosan; (c) salicylic acid/chitosan mixture (50%, w/w); (d) salicylic acid.

percentage adhesion was calculated from the difference between the platelet count before and after rotation in the glass bottle.

2.7. Cell cytotoxicity assay

THP-1 cells were cultured in RPMI1640 containing 10% FBS with antibiotics at 37 °C under 5% CO_2 for 24 h, then were seeded in a 96-well plate at a density of 8×10^4 cells/well. Samples were added to each medium as a concentration stock. After incubation for 24 h, 20 μL of MTT (5 g/L) was added to each well, followed by incubating for 4 h. DMSO (200 μL) was added to each well to dissolve any formazan crystals formed. The plates were vigorously shaken before the relative color intensity was measured at 492 nm in an Mk3 ELISA reader (Thermo Fisher Scientific, USA).

3. Results and discussion

The water-solubility of chitosan depends on its molecular weight. Generally, only the chitosan with M_w lower than 10 kD exhibits water-soluble property in neutral PH. It is worth noticing that the chitosan used in the present study is not oligosaccharide chitosan, but macromolecule biopolymer, and it is water-insoluble due to its strong crystal structure. The intermolecular hydrogen bonds play an essential role in the formation of this crystal structure. Salicylic acid is water-insoluble too, but after introducing the salicylic acid into chitosan with high molecular weight, the crystal structure of original chitosan is destroyed significantly, resulting in the water-soluble conjugating derivative, SA-chitosan (Scheme 1).

The FT-IR spectra of chitosan, SA-chitosan, salicylic acid/chitosan mixture (50%, w/w) and salicylic acid are displayed in Fig. 1. In the spectrum of original chitosan, the remarkable bands at 1653.28 and 1599.72 cm^{-1} correspond to the C=O stretching vibrations (amide I) and N—H bending vibrations (amide II), which are assigned to the residual acetyl group of chitin. Comparing to the spectrum of pristine chitosan, the spectrum of SA-chitosan presents significant alterations. Amide I band shifts to 1632 cm^{-1} slightly, and its intensity is also increased obviously due to the formation of amide group between salicylic acid and chitosan, while amide II band moves to 1566 cm^{-1} should be attributed to the formation of new intermolecular hydrogen bonds. The new band appears at 1458 cm^{-1} which is related to the —OH of benzene ring of salicylic acid can be observed clearly. Besides, it is also noticeable that the presence of new bands at 807, 768 and 707 cm^{-1} are ascribable to the characteristic bands of benzene rig of salicylic acid (out-of-plane bending of the ring C—H bonds). Meanwhile, the band around 3380 cm^{-1} shifts to 3360 cm^{-1}, and it becomes more intense and narrow, which also indicates that salicylic acid has been introduced onto chitosan due to the formation of amide group and the introduction of —OH. As Fig. 1c shown, because of the internal hydrogen bonds, a distinct band of carboxyl group appears at 1657 cm^{-1}, which is different from the classical wavenumber of C=O of carboxyl group (Silverstein, Webster, & Kiemle, 2005). The weak band at 3504 cm^{-1} corresponds to the chitosan, which makes it distinct from the spectrum of pure salicylic acid. Hence, the discrepancies between spectrum of salicylic acid/chitosan mixture (50%, w/w) and spectra of SA-chitosan and chitosan are quite prominent, suggesting that chitosan is modified with salicylic acid successfully. Moreover, it can be confirmed that the salicylic acid is highly selective toward NH_2 of chitosan owing to the absence of a band at 1710–1760 cm^{-1}, the signal of *O*-acyl ester groups.

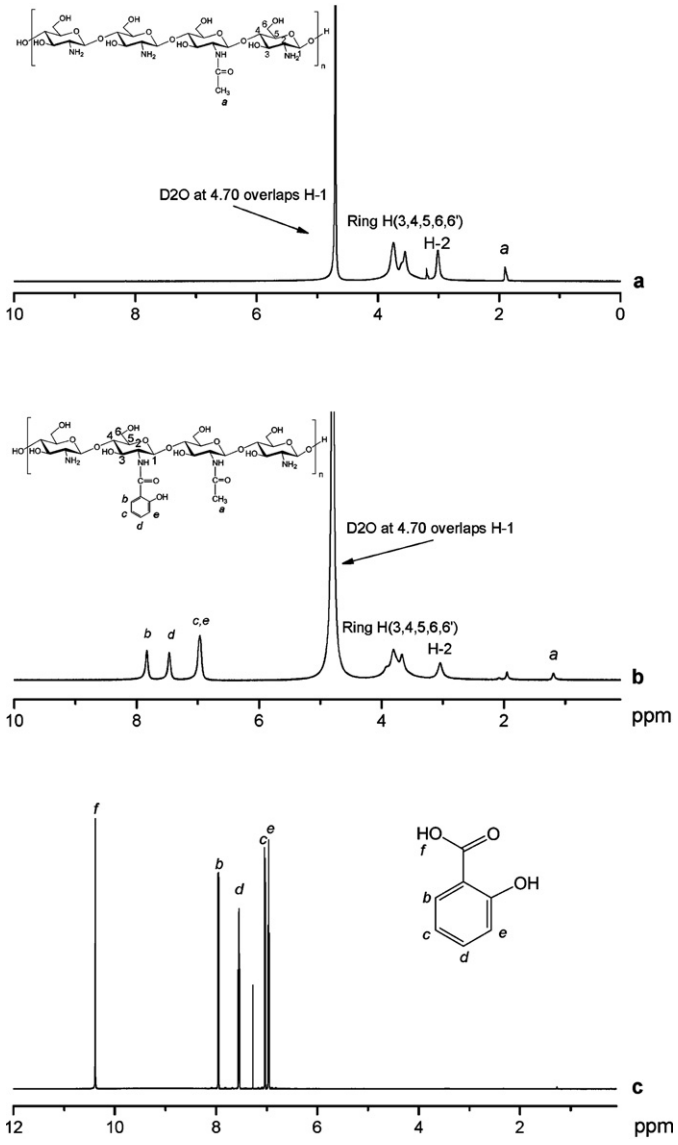

Fig. 2. ^1H NMR spectra: (a) chitosan; (b) SA-chitosan in D_2O/CCl_3COOD; (c) salicylic acid in DMSO.

The ^1H NMR spectra of chitosan, SA-chitosan and salicylic acid were shown in Fig. 2. Proton assignments for chitosan in CCl_3COOD/H_2D (Fig. 2a): $\delta_{4.70}$ to H-1 overlaps D_2O, $\delta_{3.01}$ to H-2,

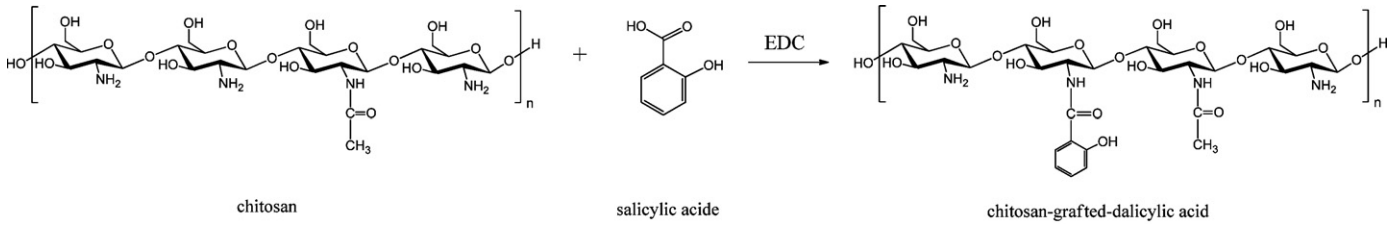

Scheme 1. Preparation route for SA-chitosan.

$\delta_{1.90}$ = NHCOC$\underline{H}_3$ (the residual acetyl groups of chitosan), $\delta_{3.47–3.74}$ to the ring protons of chitosan (H-3, 4, 5, 6, 6′). Compared to the spectrum of chitosan, the new peaks at $\delta_{6.00–8.00}$ that are attributed to the benzene ring of salicylic acid are observed in the spectrum of SA-chitosan (Prudencio, Schmeltzer, & Uhrich, 2005). While the sharp peak at $\delta_{10.38}$ that corresponds to the carboxyl groups in the spectrum of salicylic acid, disappears in the spectrum of SA-chitosan due to the fact that the carboxyl groups of salicylic acid participated in the formation of new amido bond between chitosan and salicylic acid. However, the peak of amido bond is hardly observed in view of the deuterium exchange. In addition, substitution degree of salicylic acid calculated by the ^{1}H NMR spectrum of SA-chitosan is 70.8%.

The impacts of the conjugation with salicylic acid on the thermal stability of chitosan were investigated by thermogravimetry test, and the thermogravimetry (TG) curves of chitosan and SA-chitosan are shown in Fig. 3. Both the first stage of chitosan (20.17–134.17 °C) and SA-chitosan (20.88–110.88 °C) corresponding to the weight loss of 4.88% and 4.02%, respectively, are ascribable to the evaporation of water the samples contain. However, it can be obviously observed that in the region of 130–190 °C which is the common slight slope segment of the second stage of samples, the weight loss of chitosan (0.41%) is significantly smaller than that of SA-chitosan (0.71%) because this process is the decomposition of small molecular segments, including acetyl group and aromatic group, and the amount of aromatic group is larger than that of acetyl group. Subsequently, both chitosan and SA-chitosan display the fast weight loss process in the third stage, which is attributed to the complicated process, such as the dehydration of saccharide rings, depolymerization, and decomposition of the units of the polymer (Zhang, Ping, Zhang, & Shen, 2003).

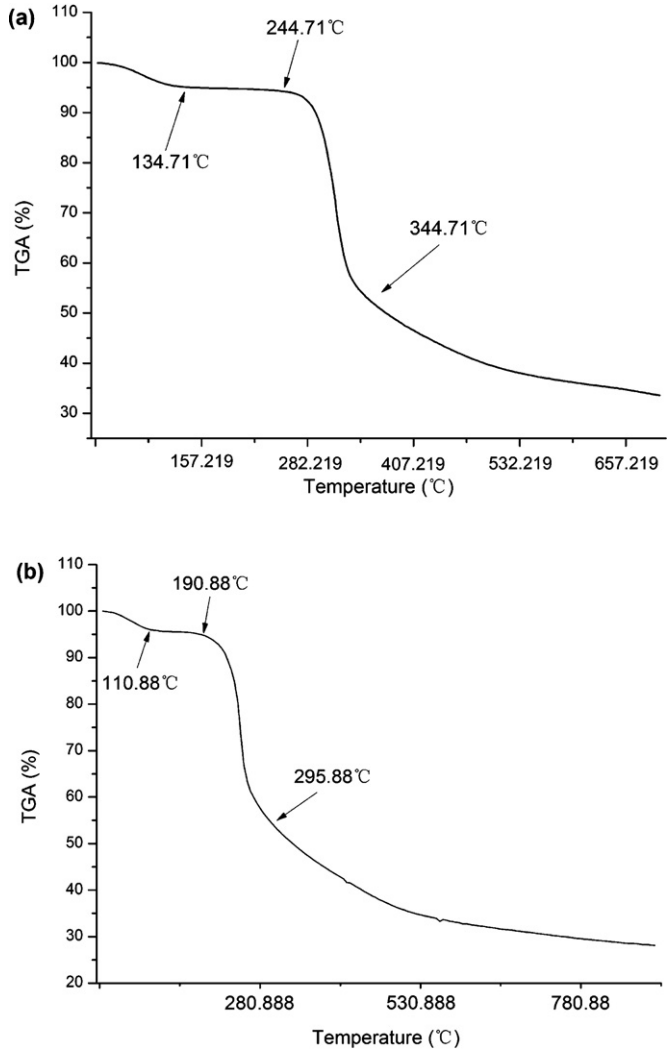

Fig. 3. TG curves: (a) chitosan; (b) SA-g-CS.

As anticipated, in Fig. 3, the temperature range during the second stage in TG curve of SA-chitosan (110–190 °C) (Fig. 3b) is narrow than that of chitosan (134–244 °C) (Fig. 3a), resulting from the less effective intermolecular interactions that the SA-chitosan contains, especially the hydrogen bonds. These results reveal that the crystalline structure of original chitosan is destroyed, and thus reduces the thermal stability. Meanwhile, the result is also confirmed by the FTIR analysis. In the spectrum of SA-chitosan, the band around 3380 cm^{-1} shifts to 3360 cm^{-1} (a lower wavenumber) (Prashanth, Kittur, & Tharanathan, 2002).

Once the crystal structure of chitosan is disrupted, SA-chitosan becomes amorphous and water-soluble, and the aromatic ring of salicylic acid serves as the hydrophobic group to decrease the surface free energy (Liu, Chen, Chen, & Liu, 2009), while the ionized free NH_2 groups act as the hydrophilic groups, resulting in strong self-aggregate ability of SA-chitosan. The self-aggregation behavior of surfactant and polymer micelles are investigated by employing pyrene as fluorescence probe by virtue of its poor solubility and sensitivity of fluorescent spectra in the presence of various concentrations of polymer solution. Considering its sensitivity of fluorescent spectra, the CAC value can be determined by the interception of two straight lines of the intensity ratio of I_{372}/I_{383} (Fig. 4) (Whihelm et al., 1991).

It is obvious that the values of I_{372}/I_{383} decline slightly with increasing concentration when the polymer concentrations are lower than CAC, yet the values lessen acutely as the concentration reached the CAC. Hence, the threshold displays that the CAC value of SCCS is 1.216×10^{-4} mg/mL. This CAC value of SA-chitosan is lower almost 1000 fold than that of other chitosan derivatives in previous reports such as oleic acid-conjugated chitosan (0.112 mg/mL) (Lee et al., 2011), and is also much lower than that of Cholesterol-modified glycol chitosan (CAC value: 122.3×10^{-3} mg/mL) (Yu, Li, Qiu, & Jin, 2008). CAC is an essential criterion to predict the stability of micelles. The lower the value of CAC, the higher stability the micelles possess, and only the micelles with low CAC value can survive for a long term in blood (Rangel-Yagui, Junior, & Tavares, 2005). A low CAC value indicates that SA-chitosan has a potent capability of self-aggregation and the excellent colloidal stability in aqueous solution. SA-chitosan can form stable nanaparticles even if in

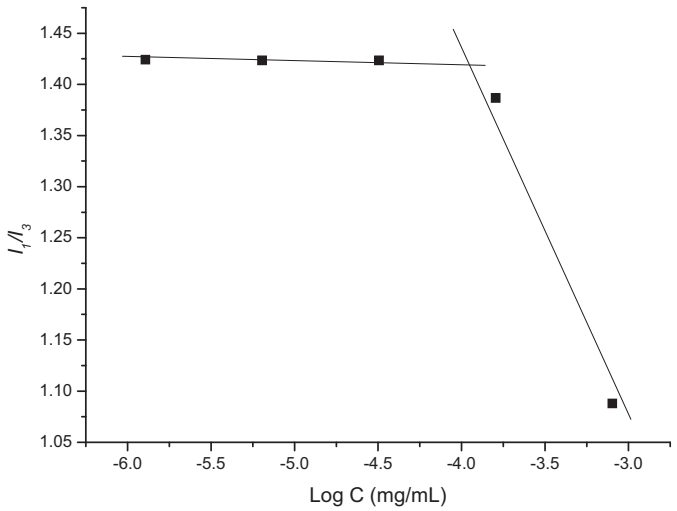

Fig. 4. Change of intensity ratio (I_{372}/I_{383}) for pyrene in water with various concentrations of SA-chitosan.

very low concentration, which is good for prolonging its circulation half-life and reducing the frequency of drug use.

The size and zeta potential of SA-chitosan micelles in an aqueous media were determined by DLS. The main size of SA-chitosan is 292 ± 2 nm and the zeta potential is 52 mV. The zeta potential values show that the SA-chitosan micelles have positive charge larger than 30 mV, which indicates that the polymeric nanoparticles have excellent dispersion stability. The positive charge of zeta potential confirms the presence of ionized amino groups at the surface of micelles.

Compared with *N*-palmitoyl chitosan (Jiang et al., 2006) which is also the hydrophobicablly modified chitosan that we reported previously, the size of the micelle of SA-chitosan is slight larger than that of *N*-palmitoyl chitosan. This might be explained by the following reasons. The substitution degree of salicylic acid is 70.8%, while that of palmitoyl chitosan is 2.0–4.0%. Although the molecular weight of aromatic ring is much smaller than that of palmitoyl group, the amount of the former is much larger than that of the later, and the former possesses the ring structure with high steric hindrance, making SA-chitosan form the larger size micelle. However, the hydrophobic chain of palmitoyl group is flexible to twist together to form more compressed hydrophobic core, resulting in the smaller size micelles.

Fig. 5 presents the morphology of SA-chitosan micelles that are depicted by TEM images. It can be observed that the shapes of nanoparticles are approximately spherical, whereas the sizes in TEM images are much smaller than that determined by DLS. This might because that the lower concentration of samples for TEM images than that for DLS, and the aggregation of micelles due to dehydration in the process of the sample preparation for TEM images. However, admittedly, the size around 300 nm that SA-chitosan formed might impact the circulation half-life in clinical, but many macromolecular drugs have the same problem. But the result of *in vitro* platelet aggregation assay indicates that the SA-chitosan can obtain the antiplatelet aggregation in a short time. However, except for the aggregation of micelles due to dehydration in the process of the sample preparation for TEM images, there might be another reason to explain phenomenon that the size determined by DLS much bigger than that of TEM images. This data is determined by DLS, in fact, the concentration of SA-chitosan in blood is very low, but this determination test required a certain concentration of SA-chitosan which was always much higher than that in clinical, so in such high concentration, more SA-chitosan molecules might get together to form bigger size. Nevertheless, the plentiful hydrophobic group causes highly strong hydrophobic interaction and forms solid core through intermolecular interaction in aqueous solution, making the micelles based on SA-chitosan stable and very compact though the size would be larger.

Table 1
Different concentration SA-chitosan on platelet aggregation in human whole blood induced by ADP (10 μM), collagen (50 mg/L) and AA (10 μM).

Group	ADP (Ω)	Collagen (Ω)	AA (Ω)
Control	5.33 ± 0.33	15.33 ± 2.73	7.33 ± 0.33
50 mg/L SA-chitosan	2.67 ± 0.33	7.67 ± 0.67	3.67 ± 0.33
20 mg/L SA-chitosan	3.33 ± 0.33	11.33 ± 0.67	6.0 ± 0.67
10 mg/L SA-chitosan	4.33 ± 0.33	13.0 ± 1.0	6.67 ± 0.33
30 mg/L SA	5.67 ± 0.33	15.33 ± 1.0	7.33 ± 0.67
Aspirin (30 mg/L)	4.0 ± 0.33	11.67 ± 0.67	5.33 ± 0.33

In the *ex vivo* platelet aggregation assay, three antiplatelet aggregation stimuli (ADP, collagen, and AA) were employed to determine the effect of SA-chitosan, aspirin and SA on platelet reactivity because - the antiplatelet aggregation is ascribable to the inhibition of platelet TXA_2 production and cyclooxygenase (Helgason et al., 1993). Besides, the amount of aspirin was set as low dose due to limitation of high aspirin dose that might cause serious side effects including mucosa irritation and blooding. The result is displayed in Table 1. SA-chitosan shows potential platelet aggregation inhibitory activity in the presence of agonists including ADP, AA and collagen. SA-chitosan (10, 20 and 50 mg/L) inhibits platelet aggregation induced by different agonists in a dose-dependent

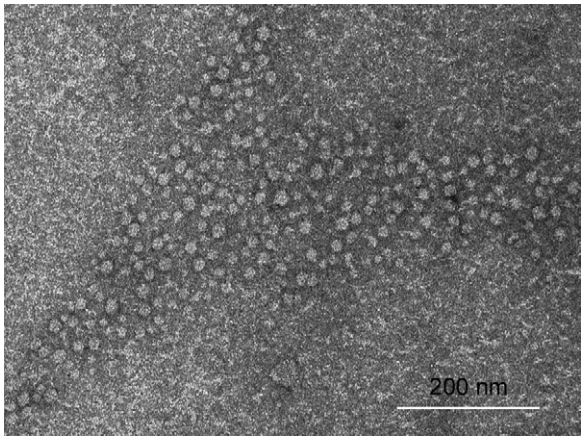

Fig. 5. TEM images of SA-chitosan nanoparticles.

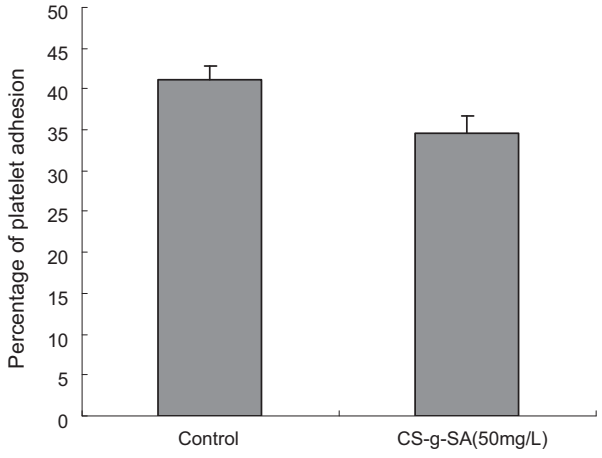

Fig. 6. Effect of SA-chitosan on the platelet adhesiveness.

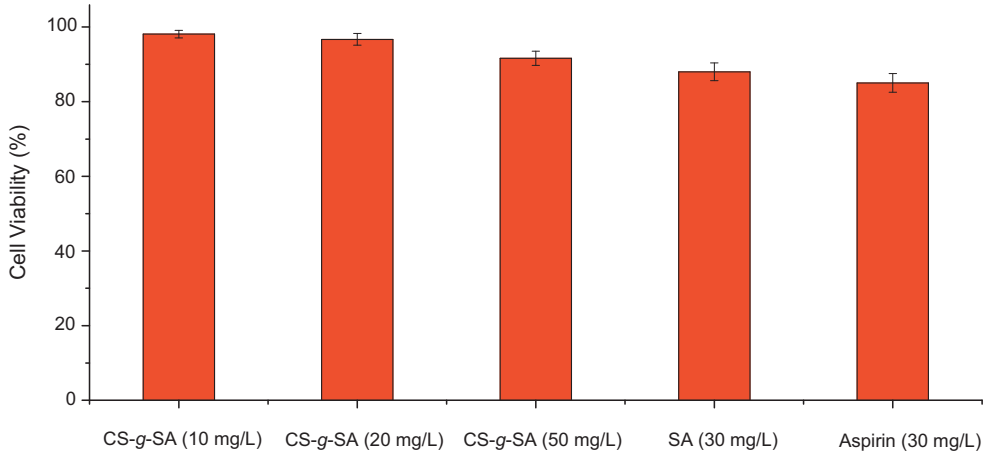

Fig. 7. Cell toxicity of different concentration of SA-chitosan on THP-1 cells after 24 h.

manner. As the reference drug, aspirin (30 mg/L) shows significant inhibition ability. And SA-chitosan is able to reduce the platelet aggregation. Moreover, it is obvious that even if the concentration of SA-chitosan (10, 20 mg/L) is lower than that of aspirin (30 mg/L), the ability of antiplatelet aggregation of SA-chitosan is equal, even higher than that of aspirin. In other word, the nanomicelles SA-chitosan have the clinical potential that its effective dosage is lower than that of low-dose aspirin to achieve the same, even better effect in terms of the function of antiplatelet aggregation, and prolonging its antiplatelet aggregation effect.

The results of the effect of SA-chitosan on the platelet adhesiveness, shown in Fig. 6, demonstrate that in the presence of SA-chitosan (50 mg/L), the percent of adhesive platelets is 34.7 + 2.0% compared with values of 41.1 + 1.8% obtained from control sample. The statistical analysis indicates a significant difference between the effect of SA-chitosan and that of untreated control ($p < 0.05$).

The cytotoxicity of samples was determined by MTT assay on THP-1 cells. The result presented in Fig. 7 shows the cell viability upon treatment with increasing concentrations of test samples after 24 h. The cell viability with 10 mg/L and 20 mg/L of SA-chitosan are 98.1 ± 1% and 96.7 ± 1.6%, while the cell viability with 50 mg/L of SA-chitosan is 91.6 ± 1.9%. Therefore, with less than 50 mg/L, these samples display no apparent cytotoxicity as compared with the control cells, while the SA-chitosan with high concentration (50 mg/L) shows only low cell cytotoxicity. However, increasing cytotoxicity is observed in cells treated with SA (30 mg/L) and aspirin (30 mg/L). It is obvious that the cytotoxicity of SA is declined drastically after modifying the chitosan. On the other hand, it is noticed that the cytotoxicity of aspirin is more potent than SA, thus taking aspirin for a long time might cause some unfavorable side-effects. As mentioned above, the results also suggest that SA-chitosan (10, 20 mg/L) performs equal, even better ability of antiplatelet aggregation than aspirin (30 mg/L) does, but without cell cytotoxicity. Hence, it can be potentially used as a safe agent.

The inhibition rates of SA-chitosan (50 mg/L) on platelet aggregation and adhesion are approximately 50% and 17%, respectively. The data suggest that it has a good inhibitor role on platelet aggregation while the effect on the platelet adhesion is not strong. However, the drug shows a good safety under these concentrations. On the other hand, though the inhibition effect on platelet adhesion at concentration of 50 mg/L is not strong, it presents a significant difference ($p = 0.015$). Conversely, excessive inhibition on platelet adhesion can induce bleeding, which would affect the safety of the drugs.

In antiplatelet aggregation assay, it is noticeable that the salicylic acid does not have antiplatelet aggregation property, while the SA-chitosan has. This might be ascribable to that the structure of SA-chitosan resembles to aspirin because there are aromatic ring and acetyl group that are the character of aspirin in the SA-chitosan. Generally, it can be explained that the aspirin reduces the platelet aggregation through inhibition of platelet cyclooxygenase, resulting in a depressant of thromboxane A_2 (Vane, Anggard, & Botting, 1990). But Szczeklik, Krzanowski, Gora, and Radwan (1992) pointed out that in terms of aspirin, the antiplatelet aggregation function might affect thrombin generation, yet it was more likely that it was unrelated to its inhibition of platelet cyclooxygenase. Hence, there might be different paths that aspirin affects the platelet. The exact path that the SA-chitosan affects the platelet is under future investigation.

4. Conclusions

Chitosan which was modified with salicylic acid (SA-chitosan), an amphiphilic chitosan derivative that possessed both antiplatelet aggregation and antiplatelet adhesion properties, was prepared successfully. Both chitosan (macromolecule biopolymer) and SA was insoluble, however, SA-chitosan was soluble after chemical modification. The substitution degree of salicylic acid was 70.8%. The nanoparticles can self-aggregate to form stable nanoparticles, its critical aggregation concentration (CAC) value was 1.216×10^{-4} mg/mL and the zeta potential was 52 mV, suggesting that the nanoparticles possessed excellent potential dispersion stability. The result of *in vitro* antiplatelet activity revealed that potential platelet aggregation inhibitory activity of SA-chitosan by different agonists in a dose-dependent manner. The platelet adhesion test showed the significant difference between the effect of SA-chitosan and that of untreated control ($p < 0.05$). *In vitro* platelet aggregation assay and platelet adhesion test revealed that SA-chitosan had excellent antiplatelet aggregation property and good ability to reduce platelet adhesion. The cell cytotoxicity assay suggested that these SA-chitosan displayed no apparent cytotoxicity as compared with the control cells. These results indicated that SA-chitosan can be potentially used as a safe antiplatelet aggregation and antiplatelet adhesion agent, and it can also be potentially employed as a potent potential polymer–drug conjugate for some blood diseases or preventing formation of thrombosis as aspirin does, but can reduce the drug frequency and dosage comparing with aspirin.

Acknowledgments

This research is supported by Natural Science Foundation of China (20874032), Postdoctoral Science Foundation of China

(20100480834) Team Program of Natural Science Foundation of Guangdong Province, China (S2011030003134), Science and Technology Planning Project of Guangdong Province, China (2008B030301202, 2010B031100014) and Key Laboratory of Medicinal Chemical Resources and Molecular Engineering (Ministry of Education) (07109001-17).

References

Bryers, J. D., Jarvis Rebecca, A., Lebo, J., Prudencio, A., Kyriakides, T. R., & Uhrich, K. (2006). Biodegradation of poly(anhydride-esters) into non-steroidal anti-inflammatory drugs and their effect on *Pseudomonas aeruginosa* biofilms in vitro and on the foreign-body response in vivo. *Biomaterials*, *27*, 5039–5048.

Helgason, C. M., Tortorice, K. L., Winkler, S. R., Penney, D. W., Schuler, J. J., McClelland, T. J., et al. (1993). Aspirin response and failure in cerebral infarction. *Stroke*, *24*, 345–350.

Jiang, G. B., Quan, D., Liao, K., & Wang, H. (2006). Novel polymer micelles prepared from chitosan grafted hydrophobic palmitoyl groups for drug delivery. *Molecular Pharmacology*, *3*, 152–160.

Kumar, M. N. V. R. (2000). A review of chitin and chitosan applications. *Reactive & Functional Polymers*, *46*, 1–27.

Kumar, R., Chen, M. H., Parmar, V. S., Samuelson, L. A., Kumar, J., Nicolosi, R., et al. (2004). Supramolecular assemblies based on copolymers of PEG600 and functionalized aromatic diesters for drug delivery applications. *Journal of the American Chemical Society*, *126*, 10640–10644.

Kumar, M. N. V. R., Muzzarelli, R. A. A., Muzzarelli, C., Sashiwa, H., & Domb, A. J. (2004). Chitosan chemistry and pharmaceutical perspectives. *Chemical Reviews*, *104*, 6017–6084.

Kwon, S. G., & Okano, T. (1996). Polymeric micelles as new drug carriers. *Advanced Drug Delivery Review*, *21*, 107–116.

Kwon, S., Park, J. H., Chung, H., Kwon, I. C., Jeong, S. Y., & Kim, I. K. (2003). Physicochemical characteristics of self-assembled nanoparticles based on glycol chitosan bearing 5 beta-cholanic acid. *Langmuir*, *19*, 10188–10193.

Lee, C. M., Jang, D. R., Kim, J., Cheong, S. J., Kim, E. M., Jeong, M. H., et al. (2011). Oleyl-chitosan nanoparticles based on a dual probe for optical/MR imaging in vivo. *Bioconjugate Chemistry*, *22*, 186–192.

Liu, K. H., Chen, B. R., Chen, S. Y., & Liu, D. M. (2009). Self-assembly behavior and doxorubicin-loading capacity of acylated carboxymethyl chitosans. *Journal of Physical Chemistry B*, *113*, 11800–11807.

Liu, T. Y., Chen, S. Y., Lin, Y. L., & Liu, D. M. (2006). Synthesis and characterization of amphiphatic carboxymethyl-hexanoyl chitosan hydrogel: Water-retention ability and drug encapsulation. *Lamgmuir*, *27*, 9740–9745.

Martin, L., Wilson, C. G., Koosha, F., Tetley, L., Gray, A. I., Senel, S., et al. (2002). The release of model macromolecules may be controlled by the hydrophobicity of palmitoyl glycol chitosan hydrogels. *Journal of Controlled Release*, *80*, 87–100.

Muzzarelli, R. A. A., Boudrant, J., Meyer, D., Manno, N., DeMarchis, M., & Paoletti, M. G. (2012). Current views on fungal chitin/chitosan, human chitinases, food preservation, glucans, pectins and inulin: A tribute to Henri Braconnot, precursor of the carbohydrate polymers science, on the chitin bicentennial. *Carbohydrate Polymers*, *87*, 995–1012.

Patrono, C., Rodriguez, L. A. G., Landolfi, R., & Baigent, C. (2005). Drug therapy-low-dose aspirin for the prevention of atherothrombosis. *New England Journal of Medicine*, *353*(22), 2373–2383.

Prashanth, K. V. H., Kittur, F. S., & Tharanathan, R. N. (2002). Solid state structure of chitosan prepared under different N-decacetylating conditions. *Carbohydrate Polymers*, *50*, 27–33.

Prudencio, A., Schmeltzer, R. C., & Uhrich, K. E. (2005). Effect of linker structure on salicylic acid-derived poly(anhydride esters). *Macromolecules*, *38*, 6895–6901.

Rangel-Yagui, C. O., Junior, A. P., & Tavares, L. C. (2005). Micellar solubilization of drugs. *Journal of Pharmacy & Pharmaceutical Science*, *8*, 147–163.

Shrivastava, S., Bera, T., Singh, S. K., Singh, G., Ramachandrarao, P., & Dash, D. (2009). Characterization of antiplatelet properties of silver nanoparticles. *ACS Nano*, *3*(6), 1357–1364.

Silverstein, R. M., Webster, F. X., & Kiemle, D. J. (2005). In D. Brennan, J. Yee, P. Kennedy, S. Wolfman-Robichaud, A. Wygal, & M. Lesure, et al. (Eds.), *Spectrometric identification of organic compounds* (7th ed., pp. 87–95). New York: John Wiley & Sons, Inc.

Szczeklik, A., Krzanowski, M., Gora, P., & Radwan, J. (1992). Antiplatelet drugs and generation of thrombin in clotting blood. *Blood*, *80*, 2006–2011.

Takahashi, S., Ushida, M., Komine, R., Shimizu, A., Uchida, T., Ishihara, H., et al. (2007). Increased basal platelet activity, plasma adiponectin levels, and diabetes mellitus are associated with poor platelet responsiveness to in vitro effect of aspirin. *Thrombosis Research*, *119*, 517–524.

Vane, J. R., Anggard, E. E., & Botting, R. M. (1990). Regulatory functions of the vascular endothelium. *New England Journal of Medicine*, *323*, 27.

Whihelm, M., Zhao, C. L., Wang, Y., Xu, R., Winnik, M. A., Mura, J. L., et al. (1991). Poly(styrene-ethyleneoxide) block copolymer micelle formation in water: A fluorescence probe study. *Macromolecules*, *24*, 1033–1040.

Wiraharma, N., Zhang, Y., Venkataraman, S., Hedrick, J. L., & Yang, Y. Y. (2009). Self-assembled polymer nanostructure delivery of anticancer therapeutics. *Nano Today*, *4*, 302–317.

Yu, J. M., Li, Y. J., Qiu, L. Y., & Jin, Y. (2008). Self-aggregated nanoparticles of cholesterol-modified glycol chitosan conjugate: Preparation, characterization, and preliminary assessment as a new drug delivery carrier. *European Polymer Journal*, *44*, 555–565.

Zhang, L., Chan, J. M., Gu, F. X., Rhee, J. W., Wang, A. Z., Radovic-Moreno, A. F., et al. (2008). Self-assembled lipid polymer hybrid nanoparticles: A robust drug delivery platform. *ACS Nano*, *2*(8), 1696–1702.

Zhang, C., Ping, Q., Zhang, H., & Shen, J. (2003). Synthesis and characterization of water-soluble O-succinyl-chitosan. *European Polymer Journal*, *39*, 1629–1634.